Cancer Cell
Article

Loss of Cutaneous TSLP-Dependent Immune Responses Skews the Balance of Inflammation from Tumor Protective to Tumor Promoting

Matteo Di Piazza,[1,3] Craig S. Nowell,[1,3] Ute Koch,[1] André-Dante Durham,[2] and Freddy Radtke[1,*]
[1]Ecole Polytechnique Fédérale de Lausanne, School of Life Sciences, Swiss Institute for Experimental Cancer Research, Lausanne, Vaud 1015, Switzerland
[2]Department of Radio-oncology, Centre Hospitalier Universitaire Vaudois, Lausanne, Vaud 1011, Switzerland
[3]These authors contributed equally to this work
*Correspondence: freddy.radtke@epfl.ch
http://dx.doi.org/10.1016/j.ccr.2012.08.016

SUMMARY

Inflammation can promote or inhibit cancer progression. In this study we have addressed the role of the proinflammatory cytokine thymic stromal lymphopoietin (TSLP) during skin carcinogenesis. Using conditional loss- and gain-of-function mouse models for Notch and Wnt signaling, respectively, we demonstrate that TSLP-mediated inflammation protects against cutaneous carcinogenesis by acting directly on CD4 and CD8 T cells. Genetic ablation of TSLP receptor (TSLPR) perturbs T-cell-mediated protection and results in the accumulation of $CD11b^+Gr1^+$ myeloid cells. These promote tumor growth by secreting Wnt ligands and augmenting β-catenin signaling in the neighboring epithelium. Epithelial specific ablation of β-catenin prevents both carcinogenesis and the accumulation of $CD11b^+Gr1^+$ myeloid cells, suggesting tumor cells initiate a feed-forward loop that induces protumorigenic inflammation.

INTRODUCTION

For many years cancer has been regarded predominantly as a cell autonomous process in which genetically transformed cells propagate the development of malignant neoplasms. However, today it is well established that tumor progression requires complex interactions between neoplastic cells and the host-derived stroma, including tumor-associated fibroblasts, niche-defining cells, and vasculature. Of critical importance is also the relationship between the tumor and the host immune system. Originally, tumor-infiltrating immune cells were thought to reflect the attempts of the immune system to eliminate cancer cells. However, today a large body of evidence indicates that malignant neoplasms can induce qualitatively distinct types of inflammation that are protumorigenic (Coussens and Werb, 2002; Hanahan and Weinberg, 2011).

Cancer-associated inflammation frequently exhibits profiles that promote both immune evasion and the growth of malignant cells. Tumors can evade T-cell-mediated clearance by skewing the acquired immune response from cytotoxic Th1 to permissive Th2 profiles (Aspord et al., 2007) or by inducing immunosuppressive regulatory T cells (Quezada et al., 2011). Tumors can also co-opt cells of the innate immune system to become constituents of the protumorigenic stroma. Notably, cells of the myeloid lineage, such as macrophages (Allavena et al., 2008) and neutrophils (Fridlender et al., 2009) can promote tumor growth by a variety of mechanisms, depending on their differentiation status. Furthermore, poorly defined immature myeloid cells can foster tumor growth directly (Kowanetz et al., 2010; Qian et al., 2011; Yang et al., 2011) or by acting as myeloid-derived suppressor cells (Gabrilovich and Nagaraj, 2009).

These data demonstrate that tumor cells modulate both acquired and innate arms of the immune system to form an integral component of the tumor stroma. The molecular basis for such immunomodulatory roles, however, is poorly defined,

Significance

Inflammatory responses that promote or inhibit cancer development are qualitatively distinct at a cellular and molecular level. In this study we show that TSLP can induce antitumorigenic inflammation by acting directly on T cells, which prevent the growth of β-catenin-dependent skin tumors. Ablation of TSLP-mediated immune responses dramatically alters the inflammatory profile, resulting in the accumulation of $CD11b^+Gr1^+$ myeloid cells that promote tumor growth by secreting Wnts. These findings provide a mechanistic explanation regarding the reduced risk of cancer in patients who suffer from allergic disorders and demonstrate a tumor protective role for TSLP. Furthermore, we reveal an additional mechanism by which tumor-associated myeloid cells can promote tumor growth.

and it is unclear to what extent oncogenes/tumor suppressors influence tumor development by such indirect mechanisms.

Mutations in the Notch signaling pathway are associated with a variety of human cancers and indicate that Notch can function as either a tumor suppressor or an oncogene (Weng and Aster, 2004). In the skin, conditional inactivation of *Notch1* in the mouse epidermis results in the development of basal/squamous cell carcinoma after chemically induced carcinogenesis (Demehri et al., 2009; Nicolas et al., 2003; Proweller et al., 2006), suggesting that Notch functions as a tumor suppressor in this tissue. In accordance, loss-of-function mutations in human Notch receptors correlate with cutaneous and lung squamous cell carcinoma (Agrawal et al., 2011; Stransky et al., 2011; Wang et al., 2011).

Factors acting downstream of Notch with respect to epithelial malignancies remain to be fully elucidated. However, deletion of *Notch1* in the murine epidermis leads to elevated levels of activated β-catenin (Nicolas et al., 2003), which has been shown to induce skin tumor formation and regulate the maintenance of $CD34^+$ cancer stem cells (Gat et al., 1998; Malanchi et al., 2008). The tumor suppressor activity of Notch signaling in the skin may therefore at least in part be due to negative regulation of the Wnt/β-catenin pathway. Whether β-catenin accumulation is due to cell autonomous deregulation or is mediated by cross-talk between different cell populations is unclear, although there is evidence for both mechanisms (Devgan et al., 2005; Kwon et al., 2011; Sanders et al., 2009).

Conditional inactivation of both *Notch1* and *Notch2* in the murine epidermis results in a chronic inflammatory condition resembling a severe form of atopic dermatitis (AD) that occurs as a consequence of elevated TSLP expression by keratinocytes (Demehri et al., 2008; Dumortier et al., 2010). This cytokine has been shown to affect a variety of cell types in the immune system and as such is believed to play a role in allergic disorders, including AD and asthma (Ziegler, 2010). Interestingly, elevated TSLP has also been associated with progression of various epithelial malignancies, including breast and pancreatic cancer (De Monte et al., 2011; Olkhanud et al., 2011; Pedroza-Gonzalez et al., 2011). In light of this, it is intriguing that loss of Notch in the skin results in increased tumor susceptibility and elevated expression of TSLP. It is presently unclear to what extent these processes are linked, although elucidation of how they interact may provide insight into how inflammation can exert either anti- or protumorigenic effects.

In this study, we have delineated the role of TSLP-mediated inflammation during skin tumorigenesis by using loss- and gain-of-function approaches for Notch and Wnt signaling, respectively.

RESULTS

Loss of TSLP Receptor Signaling in Notch Mutant Mice Results in Cutaneous Malignancy

To determine the role of TSLP in cutaneous cancer associated with loss of Notch signaling, mice carrying a $K5Cre^{ERT}$ transgene and floxed alleles of both *Notch1* and *Notch2* receptors (N1N2K5) were crossed with $Tslpr^{-/-}$ mice, thus generating $Notch1^{lox/lox}$;$Notch2^{lox/lox}$;$K5Cre^{ERT}$;$Tslpr^{-/-}$ mice (herein referred to as N1N2K5 TSLPR). This allowed us to conditionally ablate Notch signaling in the epidermis in the absence of TSLPR signaling and therefore to dissect the role of TSLP during chronic inflammation in response to Notch ablation. Consistent with our previous study, N1N2K5 mice developed an AD-like disease within 5 weeks of skin-specific inactivation of *Notch1* and *Notch2*, characterized by the degeneration of hair follicles into large cysts. N1N2K5 TSLPR mice also developed a severe skin disorder characterized by hair follicle degeneration (Figures 1A–1B; Figures S1A–S1C available online). However, in these mutants the cystic lesions could be broadly classified into two subtypes: those lined by nonproliferative epithelial cells consisting of 1–3 cell layers or larger lesions surrounded by hyperproliferative $Ki67^+$ epithelial cells (Figures 1B and 1C; Figure S1A). The hyperproliferative cystic structures in N1N2K5 TSLPR mice frequently extended deep into the underlying connective tissue of the dermis and were often visible on the surface of the skin (Figures 1A and S1B). Pathological analysis classified these hyperproliferative cysts as dysplastic lesions resembling keratoacanthomas, relatively low-grade hair follicle malignancies that can progress to invasive squamous cell carcinomas. The severity of the phenotype in N1N2K5 TSLPR animals was reflected in survival rates, as these mutants died by day 60 post-gene-inactivation (Figure 1D), most likely because of complications resulting from barrier dysfunction and tumor burden (data not shown).

These data indicate that TSLPR signaling prevents tumor formation in Notch-deficient skin. In support of this, injection of N1N2K5 mice with TSLP-neutralizing antibodies resulted in tumor development in 60% of animals (Figure S1D), thus confirming the tumor protective function of TSLP-TSLPR interactions.

The Tumor Protective Effect of TSLP Is Mediated by Hematopoietic Cells

The TSLPR is expressed by a variety of hematopoietic cells, including T, B, and dendritic cells. We therefore speculated that elevated levels of TSLP may elicit tumor protective immune responses. To confirm this, we generated bone marrow (BM) chimeras in which CD45.2 N1N2K5 hosts were reconstituted with CD45.1 $Tslpr^{-/-}$ BM prior to Notch inactivation. The reciprocal experiment was also performed, in which CD45.1 $Tslpr^{+/+}$ BM was used to reconstitute CD45.2 N1N2K5 TSLPR mice (Figure 2A). In the former, $TSLPR^{-/-}$ → N1N2K5 chimeras developed hyperproliferative dermal cysts, resembling the tumors observed in N1N2K5 TSLPR mice upon ablation of Notch signaling (Figure 2B). Conversely, N1N2K5 TSLPR mice reconstituted with $Tslpr^{+/+}$ BM were protected from tumor formation and instead developed the AD-like disease that occurs in N1N2K5 animals (Figure 2B). These data confirm that TSLPR signaling elicits antitumor responses in hematopoietic cells.

Ablation of TSLPR Signaling Alters the Inflammatory Microenvironment in Notch-Deficient Skin

The impaired antitumor immune response elicited in N1N2K5 TSLPR mice could result from either a decreased dermal inflammatory response and/or an altered inflammatory profile. To discriminate between these possibilities, we analyzed the inflammatory cells present in the dermis of both N1N2K5 and N1N2K5 TSLPR mice by flow cytometry.

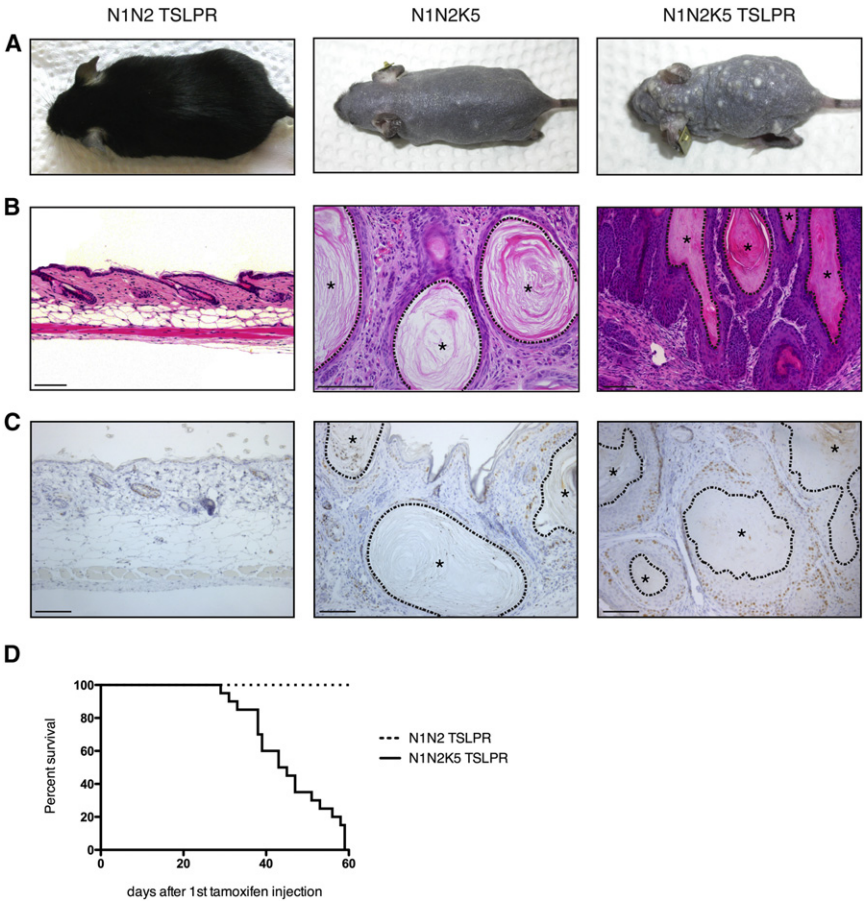

Figure 1. Loss of TSLPR Signaling in Notch-Deficient Epidermis Leads to Tumor Formation

(A) Representative images of N1N2 TSLPR control, N1N2K5, and N1N2K5 TSLPR mice 50 days after neonatal deletion of Notch.

(B and C) Representative hematoxylin and eosin (H&E) (B) and Ki67 (C) staining on dorsal skin sections of mice shown in (A). Photomicrographs in (B) are shown at different magnifications to demonstrate the hyperproliferative layers surrounding cysts (asterisks) in N1N2K5 TSLPR mice compared to N1N2K5 animals. Dotted lines mark lumen/cell border. Scale bars: 100 μm.

(D) Survival curve of N1N2 TSLPR (n = 15) and N1N2K5 TSLPR (n = 27) mice. See also Figure S1.

We noted that during the earlier stages subsequent to Notch inactivation, the inflammatory response in N1N2K5 TSLPR mice was reduced compared to N1N2K5 mutants (data not shown). However, once the macroscopic phenotype was highly overt at 4–5 weeks after Notch ablation, the proportion of dermal $CD45^+$ cells in both N1N2K5 and N1N2K5 TSLPR mice was on average 5-fold higher compared to normal littermate controls (Figure 2C). Thus, the inflammatory response in N1N2K5 and N1N2K5 TSLPR mice was quantitatively equivalent at the phenotypic endpoint.

Detailed phenotypic analysis of the dermal inflammatory infiltrates revealed several changes between N1N2K5 and N1N2K5 TSLPR mice, including alterations in the proportions of $CD117^+$ mast cells and $B220^+$ B cells (Figure 2D). However, the most striking differences were apparent in the T and myeloid cell compartments. In N1N2K5 animals, the proportion of $CD4^+$ and $CD8^+$ T cells was 12.7% and 10.4%, respectively, whereas in N1N2K5 TSLPR mice, the proportions were reduced on average to 1.8% and 1.1% (Figure 2D). In addition, $CD11b^+Gr1^+$ myeloid cells constituted just 7.2% of dermal $CD45^+$ cells in N1N2K5 mice, whereas this population increased dramatically to 36.7% upon ablation of TSLPR (Figure 2D).

Collectively, these data demonstrate that loss of TSLPR signaling in Notch-deficient epidermis results in reduced proportions of $CD4^+$ and $CD8^+$ T cells and increased infiltration of $CD11b^+Gr1^+$ myeloid cells.

TSLPR Signaling in T Cells Mediates Protection against Tumor Formation

The observation that specific populations of dermal inflammatory cells are altered quantitatively upon ablation of TSLPR signaling suggests that the cells responsible for mediating tumor protection in response to TSLP are likely to be within these compartments. Therefore, to functionally assess the role that specific cell types play in TSLP-mediated tumor protection, lethally irradiated N1N2K5 mice were reconstituted with $Tslpr^{+/+}$ BM derived from different gene targeted mice lacking specific hematopoietic cell types (Figure 2E). In this system, the development of tumors after Notch inactivation is a direct consequence of loss of a specific hematopoietic population.

We initially determined the functional contribution of lymphoid populations by reconstituting N1N2K5 mice with $Rag2^{-/-}\gamma c^{-/-}$ and $Rag2^{-/-}$ BM. In both cases, more than 90% of reconstituted N1N2K5 mice developed tumors, indicating that the protective cell type resided within the T or B cell compartment, not the NK cell population (Figures 2F and S2A). Consistent with this, 78% of the mice in which NK cells were depleted by injection of PK1.36 monoclonal antibody remained tumor free, and those mice that did develop tumors presented only mild lesions (Figure S2B). To determine if B cells were required for tumor protection, we reconstituted N1N2K5 mice with $Jh^{-/-}$ BM. In this experiment, 83% of mice were resistant to tumor formation, indicating that B cells do not mediate TSLPR-dependent tumor protection and therefore suggesting that the critical cell type resides within the T cell compartment (Figures 2F and S2A). In support of this, antibody-mediated depletion of $CD4^+$ and $CD8^+$ T cells resulted in tumor development in 83% of N1N2K5 mice (Figure S2C). To establish the role of T cells conclusively, we reconstituted N1N2K5 mice with $Cd4^{-/-}$ and $Cd8\alpha^{-/-}$ BM. In this setting, the majority of mice reconstituted with $Cd4^{-/-}$ BM were resistant to tumor formation (73%), whereas 74% of $Cd8\alpha^{-/-} \rightarrow$ N1N2K5 chimeras developed severe tumors (Figures 2F and S2A). Taken together, these data demonstrate

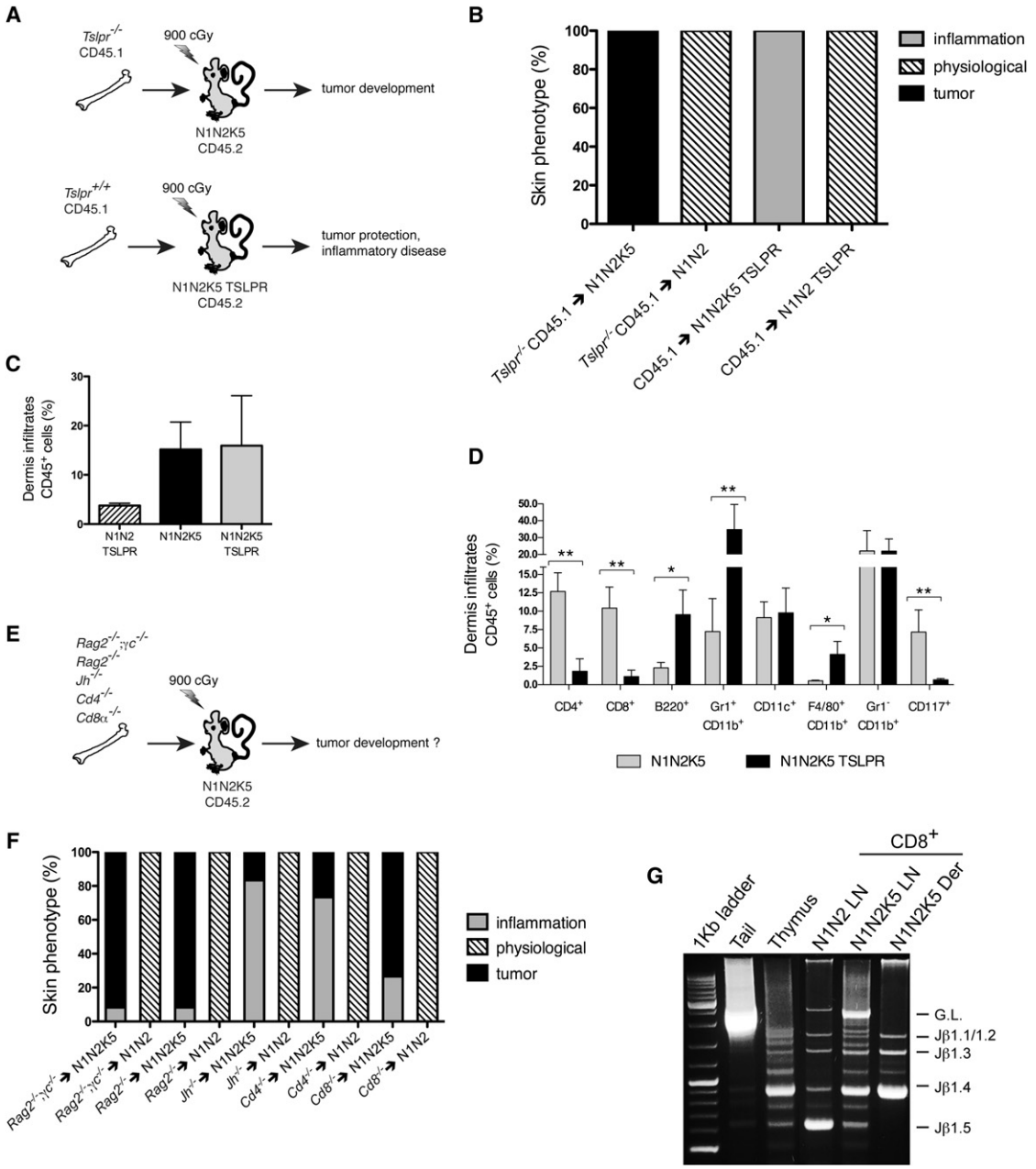

Figure 2. CD8$^+$ T Cells Are Required for TSLPR-Mediated Tumor Suppression

(A) Schematic depiction of experimental layouts. Lethally irradiated CD45.2 N1N2K5 (n = 14) and N1N2K5 TSLPR mice (n = 10) were transplanted with CD45.1 *Tslpr*$^{-/-}$ BM and CD45.1 *Tslpr*$^{+/+}$ BM, respectively, prior to ablation of Notch.

(B) Bar diagram summarizing the results of the experiments described in (A). Data represent the results of three independent experiments. N1N2 (n = 15) and N1N2 TSLPR (n = 12) littermate controls were included.

(C) Bar diagram showing the proportion of CD45$^+$ cells in the dermis of N1N2 TSLPR control, N1N2K5, and N1N2K5 TSLPR mice 4–6 weeks after deletion of Notch.

(D) Bar diagram showing the proportions of CD45$^+$ subpopulations present in the dermis of N1N2K5 and N1N2K5 TSLPR mice 4–6 weeks after deletion of Notch and development of overt skin phenotypes. (C) and (D) Dermal cell infiltrates were quantified by flow cytometry; data represent the mean of five independent experiments (mean ± SD; *p < 0.01; **p < 0.001).

(E) Schematic depiction of experimental layout. N1N2K5 and littermate mice were transplanted with BM from *Rag2*$^{-/-}$;γc$^{-/-}$ (n = 12/9), *Rag2*$^{-/-}$ (n = 12/11), *Jh*$^{-/-}$ (n = 12/7), *Cd4*$^{-/-}$ (n = 16/11), or *Cd8α*$^{-/-}$ (n = 15/10) donors.

(F) Bar diagram summarizing the combined results of six independent BM transfer experiments as depicted in (E).

(G) PCR analysis of Dβ1-Jβ1 TCR rearrangement performed on genomic DNA from CD8$^+$ T cells isolated from lymph nodes (LN) or dermis (Der). Tail and thymus were used as germline and rearranged controls, respectively. Bands corresponding to rearrangements containing Jβ1.1-Jβ1.5 are indicated. Additional bands are nonspecific. See also Figure S2.

that CD8$^+$ T cells are required to mediate the tumor-protective response elicited by TSLPR signaling. Consistent with this, analysis of TCR rearrangement in dermal CD8$^+$ T cells isolated from N1N2K5 mice revealed the predominance of Dβ1-Jβ1.4 rearrangements, suggesting that the cytotoxic T cell response is antigen specific (Figure 2G).

Previous studies have demonstrated that TSLP acts directly on CD4$^+$ (Al-Shami et al., 2005; Rochman et al., 2007) and CD8$^+$ (Rochman and Leonard, 2008) T cells during allergic immune responses. Thus, to investigate whether CD8$^+$ T cells alone or T cells in general are sufficient for tumor protection, adoptive transfer experiments were performed in which N1N2K5 TSLPR mice were injected with different combinations of WT CD4$^+$ and/or CD8$^+$ T cells (Figure 3A; Figure S3A). When CD8$^+$ or CD4$^+$ T cells were transferred alone, the proportion of recipients exhibiting tumor resistance was 65% and 90%, respectively (Figure 3B). Chimeric mice that did develop tumors upon transfer of CD4$^+$ or CD8$^+$ T cells showed reduced tumor numbers and severity compared to control mice receiving either PBS, CD11c$^+$ dendritic cells, or B220$^+$ B cells (Figures 3B and S3B; data not shown). The level of protection conferred by CD4$^+$ T cells was surprising in light of the BM reconstitution experiments described above, which indicated that CD4$^+$ T cells are dispensable for tumor protection. However, flow cytometric analysis indicated that adoptively transferred CD4$^+$ T cells induced the recruitment of host-derived CD8$^+$ T cells, thus restoring the protective cytotoxic response (Figure 3C). The highest level of protection was observed when CD4$^+$ and CD8$^+$ T cells were administered together, as recipients in these cases exhibited complete protection from tumor development (Figure 3B). Importantly, tumor protection did not occur as a consequence of inefficient gene inactivation or counterselection of Notch-deficient epidermal cells (Figures S3C and S3D).

The finding that the adoptive transfer of WT T cells can prevent tumor formation in N1N2K5 TSLPR mice indicates that T cells respond directly to TSLP and do not act in response to another TSLP responsive cell type. Consistent with this, phosphoflow cytometric analysis of pSTAT5 expression, which acts downstream of TSLPR ligation, revealed that only dermal CD4$^+$ and CD8$^+$ T cells from N1N2K5 mice are pSTAT5$^+$ (Figures 3D and S3E). Interestingly, TSLPR signaling does not appear to be required for T cell migration in vitro (Figure S3F), and thus it seems likely that its tumor-protective effect is mediated via increased T cell survival/proliferation and/or activation.

Finally, to determine if TSLP-responsive T cells could elicit protection against preformed tumors, we adoptively transferred CD4$^+$ and CD8$^+$ T cells into N1N2K5 TSLPR mice 2 weeks post-gene-inactivation and assayed tumor development (Figure 3E). Strikingly, compared to control animals receiving either CD11c$^+$ dendritic cells or B220$^+$ B cells, mice receiving both CD4$^+$ and CD8$^+$ T cells exhibited complete tumor protection (Figure 3F). Thus, TSLP-responsive T cells have the capacity to control preformed malignancies, at least during the early stages of tumor progression.

CD11b$^+$Gr1$^+$ Myeloid Cells Promote Tumor Development

As described above, a significant inflammatory component in N1N2K5 TSLPR dermis is the CD11b$^+$Gr1$^+$ myeloid population, which correlates with tumor progression. To assess if CD11b$^+$ Gr1$^+$ myeloid cells promote tumor growth in N1N2K5 TSLPR mice, we depleted Gr1$^+$ cells by intraperitoneal injection of the RB6.8C5 monoclonal antibody (Figure 4A). Depletion of Gr1$^+$ cells was confirmed by flow cytometric analysis of both peripheral blood and dermal infiltrates (Figure 4B and data not shown), and tumor progression was assessed by histology. As expected, mice receiving isotype control antibody developed large cystic tumors lined by hyperproliferative epithelial cells (Figures 4C and 4D). In contrast, mice in which Gr1$^+$ cells were depleted developed smaller cysts that were predominantly lined by epithelial cells 1–2 cell layers thick, and thus resembled the phenotype observed in N1N2K5 mice (Figures 4C and 4D).

The above data indicated that CD11b$^+$Gr1$^+$ myeloid cells perform a functional role in promoting tumor development. This observation may reflect myeloid-derived suppressor cell activity, in which antitumor T cell responses are suppressed, or may be due to the promotion of tumor growth in a more direct manner. To distinguish between these possibilities, we isolated CD11b$^+$Gr1$^+$ myeloid cells from the tumor-associated microenvironment of N1N2K5 TSLPR mice and assessed their ability to suppress T cell activation in vitro. We could not detect any effect of CD11b$^+$Gr1$^+$ myeloid cells on the proliferation of either CD4$^+$ or CD8$^+$ T cells (Figure 4E). Accordingly, depletion of CD11b$^+$Gr1$^+$ cells did not result in an increase of dermal T cells in N1N2K5 TSLPR mice (Table S1). These data therefore suggest that the CD11b$^+$Gr1$^+$ population does not perturb T cell responses but rather promotes tumor growth directly.

Tumor Formation in the Absence of TSLPR Signaling Is β-Catenin Dependent

The macroscopic phenotype presented in N1N2K5 TSLPR mice is reminiscent of extracolonic manifestations presented in patients with familial adenomatous polyposis (FAP), in which loss-of-function mutations in the *APC* gene result in constitutive activation of the Wnt/β-catenin pathway (Jagelman, 1991). Elevated β-catenin-mediated signaling is also implicated in a variety of skin cancers (Gat et al., 1998; Malanchi et al., 2008). The link between Wnt/β-catenin signaling and cancer therefore prompted us to investigate the status of β-catenin in N1N2K5 TSLPR mice.

Immunohistochemistry (IHC) for active β-catenin was performed on skin sections from N1N2K5, N1N2K5 TSLPR, and N1N2 TSLPR control mice. In N1N2K5 TSLPR mutants, active β-catenin was present in the majority of hyperproliferative cysts, in contrast to N1N2K5 mice, where it was largely absent (Figure 5A). These data suggest a role for β-catenin in the development and/or maintenance of skin tumors in these animals.

To investigate whether β-catenin is functionally required for tumor development, we generated *Notch1*$^{lox/lox}$;*Notch2*$^{lox/lox}$;*Ctnnb1*$^{lox/lox}$;*K5Cre*^{ERT} *Tslpr*$^{-/-}$ mice (hereafter N1N2βcatK5 TSLPR), in which *Notch1*, *Notch2*, and the β-catenin gene (*Ctnnb1*) can simultaneously be deleted in the skin (Figures S4A and S4B). Strikingly, ablation of β-catenin prevented the formation of cystic tumors in N1N2βcatK5 TSLPR mice, establishing that tumor development in these animals is β-catenin dependent (Figure 5B). Flow cytometric analysis of dermal infiltrates in N1N2βcatK5 TSLPR mice revealed increased infiltration of CD45$^+$ cells compared to littermate control animals,

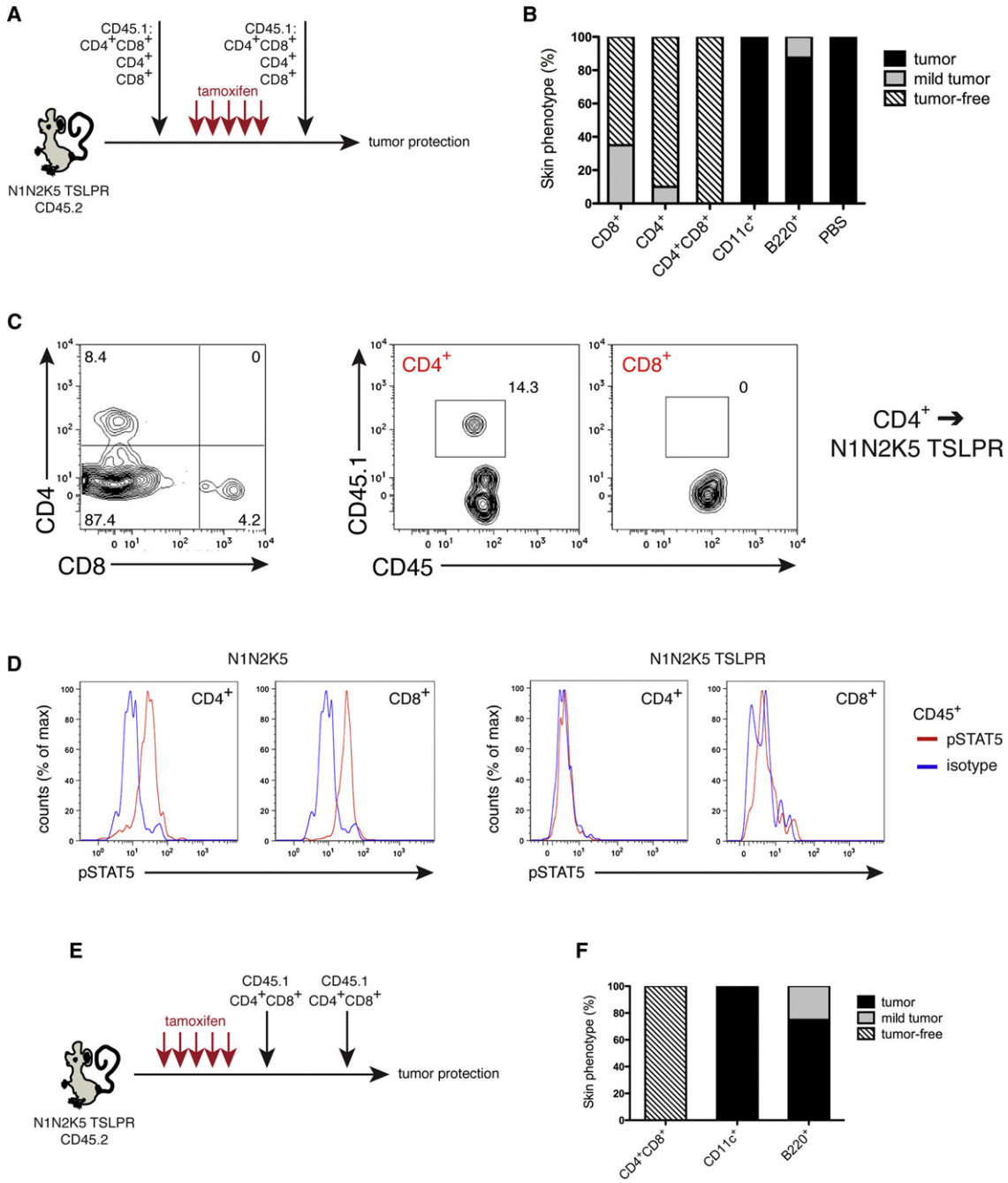

Figure 3. T Cells Are Sufficient to Mediate TSLP-Dependent Tumor Protection

(A) Schematic depiction of experimental layout. N1N2K5 TSLPR mice were transplanted with 10^7 CD45.1$^+$ immune cells in the following combination: CD11c$^+$ cells (n = 3), B220$^+$ B cells (n = 8), CD4$^+$ T cells (n = 14), CD8$^+$ T cells (n = 16), and CD4$^+$ and CD8$^+$ T cells (n = 8). One N1N2K5 TSLPR mouse injected with PBS was included as a positive control in each experiment (n = 5).

(B) Bar diagram showing the results of the experiment described in (A). Data represent the results of five independent experiments.

(C) Representative flow cytometric analysis of dermal T cells in a N1N2K5 TSLPR mouse adoptively transferred with WT CD45.1 CD4$^+$ T cells. (Left) Shows proportions of CD4$^+$ and CD8$^+$ T cells in dermal inflammatory infiltrates. (Middle and Right) Shows contribution to CD4$^+$ and CD8$^+$ T cells by donor-derived (CD45.1) cells respectively.

(D) Flow cytometric analysis of pSTAT5 expression in CD4$^+$ and CD8$^+$ T cells in the dermis of N1N2K5 and N1N2K5 TSLPR mice. Analysis was performed 5 weeks after Notch inactivation, when animals displayed an overt skin phenotype.

(E) Schematic depiction of experimental layout. Notch signaling was ablated in N1N2K5 TSLPR mice. Two weeks post-gene-inactivation, animals were transplanted with 10^7 CD11c$^+$ cells (n = 2), B220$^+$ B cells (n = 3), or CD4$^+$ and CD8$^+$ T cells (n = 5) from CD45.1 donors.

(F) Bar diagram showing the combined results of two independent experiments (described in E).

See also Figure S3.

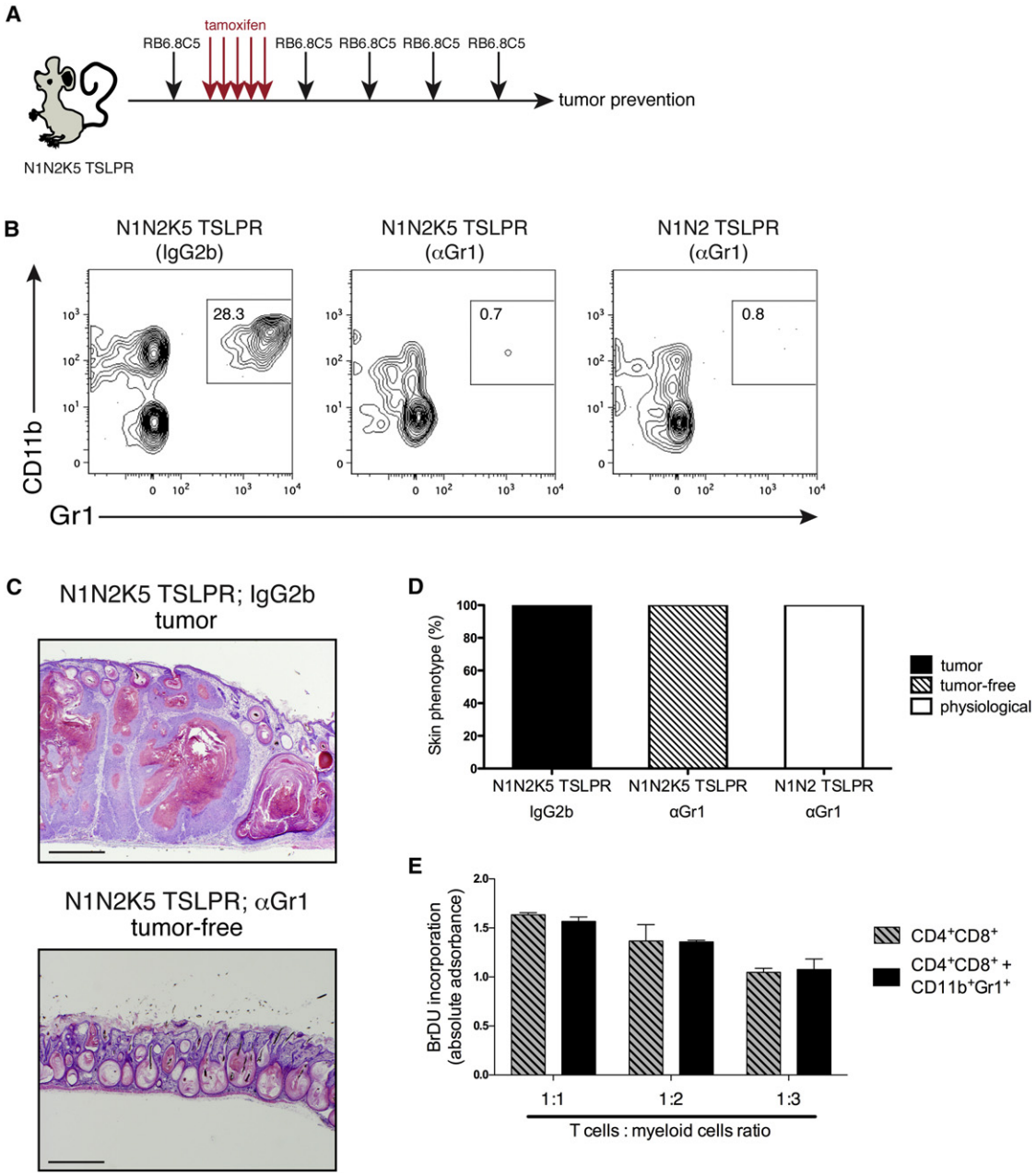

Figure 4. CD11b$^+$Gr1$^+$ Myeloid Cells Promote Tumor Development in N1N2K5 TSLPR Mice

(A) Schematic depiction of experimental layout. N1N2K5 TSLPR mice (n = 11) and N1N2 TSLPR littermate controls (n = 8) were injected with αGr1 antibody (RB6.8C5) to deplete Gr1$^+$ myeloid cells. Administration of αGr1 was initiated 2 days prior to deletion of Notch (induced by five consecutive tamoxifen injections starting at P30) and subsequently every 5 days after the final tamoxifen injection. IgG2b isotype control antibody was also administered to N1N2K5 TSLPR mice (n = 4) and N1N2 TSLPR littermates (n = 2; data not shown). Analysis was performed 7 weeks after Notch inactivation.

(B) Representative flow cytometric analysis of CD11b$^+$Gr1$^+$ myeloid cells in the dermis of N1N2K5 TSLPR mice injected with IgG2b or αGr1 antibody.

(C) Representative H&E staining performed on dorsal skin sections of N1N2K5 TSLPR mice receiving IgG2b isotype control antibody (top) or αGr1 (bottom). Scale bars: 400 μm.

(D) Bar diagram summarizing the results of the experiment described in (A). Data represent the results of three independent experiments.

(E) Bar diagram showing the results of in vitro T cell suppression assay. Immunosuppressive activity of myeloid cells was assayed by coculturing splenic C57BL/6 T cells with CD45$^+$CD11b$^+$Gr1$^+$ cells isolated from tumor-bearing N1N2K5 TSLPR skin in the ratios indicated. Myeloid cell numbers were kept constant (3.6×10^4 cells/well), and T cell numbers were reduced appropriately to adjust the T cell:myeloid cell ratio. BrdU incorporation was determined by measuring absorbance after 72 hr of coculture. Data represents the results of three independent experiments (mean ± SD).

See also Table S1.

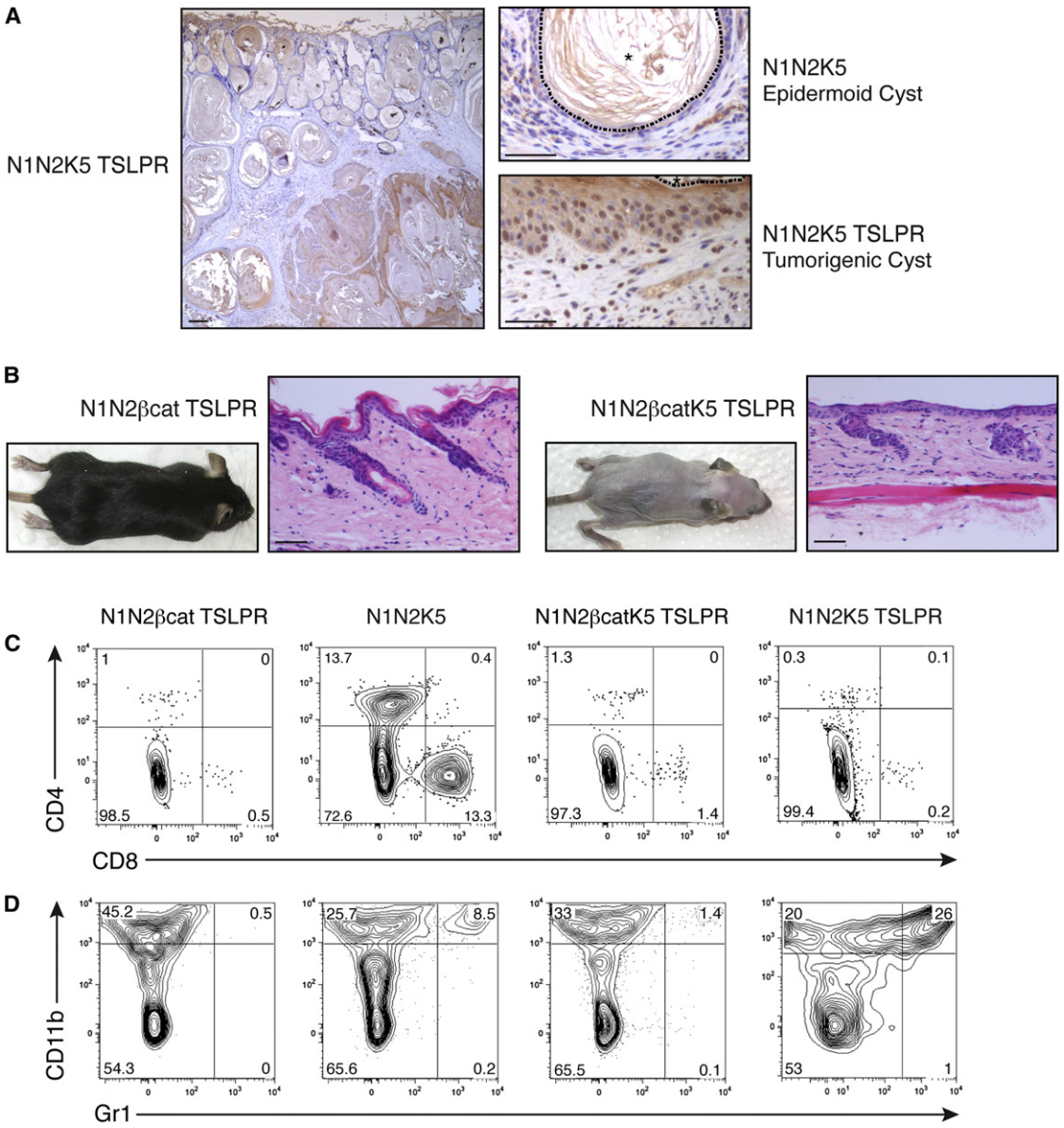

Figure 5. Tumor Formation in N1N2K5 TSLPR Mice Is β-Catenin Dependent

(A) Representative IHC staining for active β-catenin on skin sections from N1N2K5 TSLPR and N1N2K5 mice. Genotypes are indicated beside each image. (Left) Shows low magnification image of N1N2K5 TSLPR skin. (Right) Show high magnification of epithelial cells lining degenerative cysts. Asterisks demarcate single cysts; dotted lines mark lumen/cell border.

(B) Representative photographs and H&E staining of N1N2βcatK5 TSLPR mice and littermate controls 65 days after gene inactivation. In all experimental settings gene inactivation was performed by five consecutive daily tamoxifen injections starting at day P6.

(C and D) Representative flow cytometric analysis of dermal $CD4^+$ and $CD8^+$ T cells (C) and $CD11b^+Gr1^+$ myeloid cells (D) in N1N2βcat TSLPR, N1N2K5, N1N2βcatK5 TSLPR, and N1N2K5 TSLPR mice. Scale bars: 200 μm.

See also Figure S4.

confirming that in this context epidermal deletion of Notch continued to elicit a chronic inflammatory response (Figure S4C). Consistent with the absence of TSLPR, $CD4^+$ and $CD8^+$ T cells represented less than 3% of dermal $CD45^+$ cells (Figure 5C). Importantly, serum levels of TSLP remained elevated despite the loss of β-catenin (Figure S4D).

Interestingly, the accumulation of dermal $CD11b^+Gr1^+$ myeloid cells was impaired in N1N2βcatK5 TSLPR mice (Figure 5D), indicating that the recruitment and/or development of this population is independent of TSLP but dependent on epithelial-specific Wnt/β-catenin signaling.

$CD11b^+Gr1^+$ Myeloid Cells Promote Tumor Development by Provision of Wnt Ligands

Having established that β-catenin signaling is required for cutaneous tumor development in N1N2K5 TSLPR mice, we next

addressed how increased Wnt signaling is mediated. Initially, we determined if Wnt ligand expression was upregulated in N1N2K5 TSLPR mice by performing real-time PCR on whole skin. This analysis revealed that compared to normal skin isolated from N1N2 TSLPR mice, skin from N1N2K5 TSLPR mutants displayed increased expression of a variety of Wnt ligands, including *Wnt3a*, *Wnt4*, *Wnt10a*, and *Wnt10b* (Figure 6A). We then addressed the cellular source of Wnts by performing real-time PCR on fluorescence-activated cell sorting (FACS)-purified cell populations isolated from tumor-bearing N1N2K5 TSLPR dermis. For this analysis, we focused our attention on $CD11b^+$ $Gr1^+$ myeloid cells, as these cells are required for tumor development in N1N2K5 TSLPR mice and accumulate in the tumor stroma. Wnt ligand expression was also assessed in tumor-associated $CD11b^+Gr1^-$ cells and fibroblasts isolated from N1N2K5 TSLPR mice, as well as normal dermal fibroblasts isolated from N1N2 TSLPR controls. Interestingly, all cell types isolated from N1N2K5 TSLPR tumors exhibited increased expression of Wnt ligands compared to normal dermal fibroblasts (data not shown). However, comparison of the different tumor-associated populations demonstrated that the highest levels of Wnt ligand expression were detected in $CD11b^+Gr1^+$ myeloid cells, particularly with respect to *Wnt3a*, which exhibited a 40-fold increase in expression compared to tumor-associated fibroblasts (Figure 6B). To confirm that $CD11b^+Gr1^+$ myeloid cells produced WNT3A protein, we performed immunofluorescent (IF) staining on skin sections isolated from N1N2K5 TSLPR and N1N2K5 mice. Consistent with the gene expression analysis, WNT3A colocalized with $Gr1^+$ myeloid cells, which were frequently located in close proximity to epithelial tumor cells (Figure 6C). In N1N2K5 dermis, $Gr1^+$ cells were only rarely detected, although those that were present were also $WNT3A^+$ (Figure 6C and data not shown). We also analyzed WNT3a expression by western blot in tumor-bearing and non-tumor-bearing regions of N1N2K5 TSLPR skin and correlated this data with the proportions of $CD11b^+Gr1^+$ myeloid cells present. Consistent with our previous observations, the highest levels of WNT3a expression were detected in tumor-bearing regions of skin containing high proportions of $CD11b^+Gr1^+$ myeloid cells (Figure 6D; Figures S5A–S5C). We also observed WNT3A expression in cystic epithelial cells in both N1N2K5 and N1N2K5 TSLPR skin (Figure 6C; Figure S5B), indicating that $CD11b^+Gr1^+$ myeloid cells are not the exclusive source of this protein.

These data suggest that the elevated Wnt/β-catenin signaling observed in N1N2K5 TSLPR skin tumors is at least in part mediated by $CD11b^+Gr1^+$ myeloid cells. To explore this possibility further, we performed a coculture assay using a Tcf-luciferase reporter cell line (Tcf-Luc) in conjunction with myeloid cells and/or fibroblasts isolated from tumor-bearing N1N2K5 TSLPR skin. Coculture with $CD11b^+Gr1^+$ cells or fibroblasts alone did not induce luciferase activity in the Tcf-Luc cells. However, when used in combination, $CD11b^+Gr1^+$ cells and tumor fibroblasts induced a significant 2.5-fold increase in luciferase activity compared to Tcf-Luc cells cultured alone (Figure 6E), indicating that these cells have the functional capacity to induce Wnt/β-catenin signaling in neighboring cells. The requirement of tumor-associated fibroblasts likely reflects the expression of potentiating factors by these cells, as we observed markedly increased expression of the Wnt-potentiator Periostin (POSTN) (Malanchi et al., 2012) in the stroma of N1N2K5 TSLPR dermis (Figure S5D).

Collectively, these data indicate that the accumulation of $CD11b^+Gr1^+$ myeloid cells in N1N2K5 TSLPR mice results in promotion of tumor growth by increased provision of Wnt ligands. In support of this conclusion, depletion of $CD11b^+Gr1^+$ cells from the dermis of N1N2K5 TSLPR mice using the RB6.8C5 antibody results in reduced nuclear β-catenin staining in epidermal cysts (Figure S5E).

TSLPR Signaling Mediates Tumor Protection in Notch-Independent Skin Cancers

We next sought to determine if TSLP signaling could mediate tumor protection in other models of skin cancer in which Notch expression/signaling is maintained in the epidermis. To this end, we utilized $Ctnnb1^{lox(ex3)};K5Cre^{ERT}$ mice (hereafter βcatΔ3K5), in which constitutively active β-catenin can be induced in the epidermis by conditionally deleting exon3 of the β-catenin gene (Harada et al., 1999). In this model, activation of β-catenin results in the formation of hair-follicle-derived tumors over a period of several months (Gat et al., 1998). We subsequently generated βcatΔ3K5 mice lacking TSLPR (βcatΔ3K5 TSLPR) and induced expression of the dominant active mutant of β-catenin. In agreement with previous reports, βcatΔ3K5 mice developed mild skin phenotypes at 75 days post-gene-induction (Gat et al., 1998), presenting as cystic hair-follicle-derived tumors (Figure 7A). In contrast, βcatΔ3K5 TSLPR mutants developed overtly more severe phenotypes within 25 days of β-catenin induction, exhibiting extensive hair loss and thickening of the skin (Figure 7A). When analyzed histologically, cystic tumors were prevalent and were significantly larger than those observed in βcatΔ3K5 mice (Figures 7A and 7B), which at this time point had not developed a severe skin phenotype. The difference in phenotypic severity between the TSLPR-deficient and competent mice was reflected in survival rates, with 80% of βcatΔ3K5 TSLPR animals succumbing within 30 days of β-catenin induction. By contrast, all βcatΔ3K5 mice survived beyond 60 days (Figure S6A). Importantly, TSLP serum levels were increased in both βcatΔ3K5 and βcatΔ3K5 TSLPR animals compared to littermate controls (Figure 7C). Moreover, analysis of dermal inflammatory cells revealed that $CD4^+$ and $CD8^+$ T cells were significantly reduced in $Tslpr^{-/-}$ compared to $Tslpr^{+/+}$ control mutants (Figure 7D), supporting the hypothesis that TSLP mediates protection from cutaneous tumors by promoting T-cell-mediated immunity.

Interestingly, we also observed accumulating $CD11b^+Gr1^+$ populations in the cutaneous tumors arising in βcatΔ3K5 TSLPR mice (Figure 7D). In this system β-catenin signaling is activated in the epithelium autonomously and thus the effects of Wnt-driven tumorigenesis should be independent of stromal derived ligands. To confirm this, we depleted $CD11b^+Gr1^+$ cells in βcatΔ3K5 TSLPR mice by intraperitoneal injection of RB6.8C5 and assessed tumor development upon gene activation. Consistent with our hypothesis, tumor development in these animals was not adversely affected by the depletion of $Gr1^+$ myeloid cells (Figures S6B–S6D).

Taken together, these results suggest that TSLPR-mediated inflammation protects against different forms of cutaneous tumors. In support of this conclusion, the accompanying

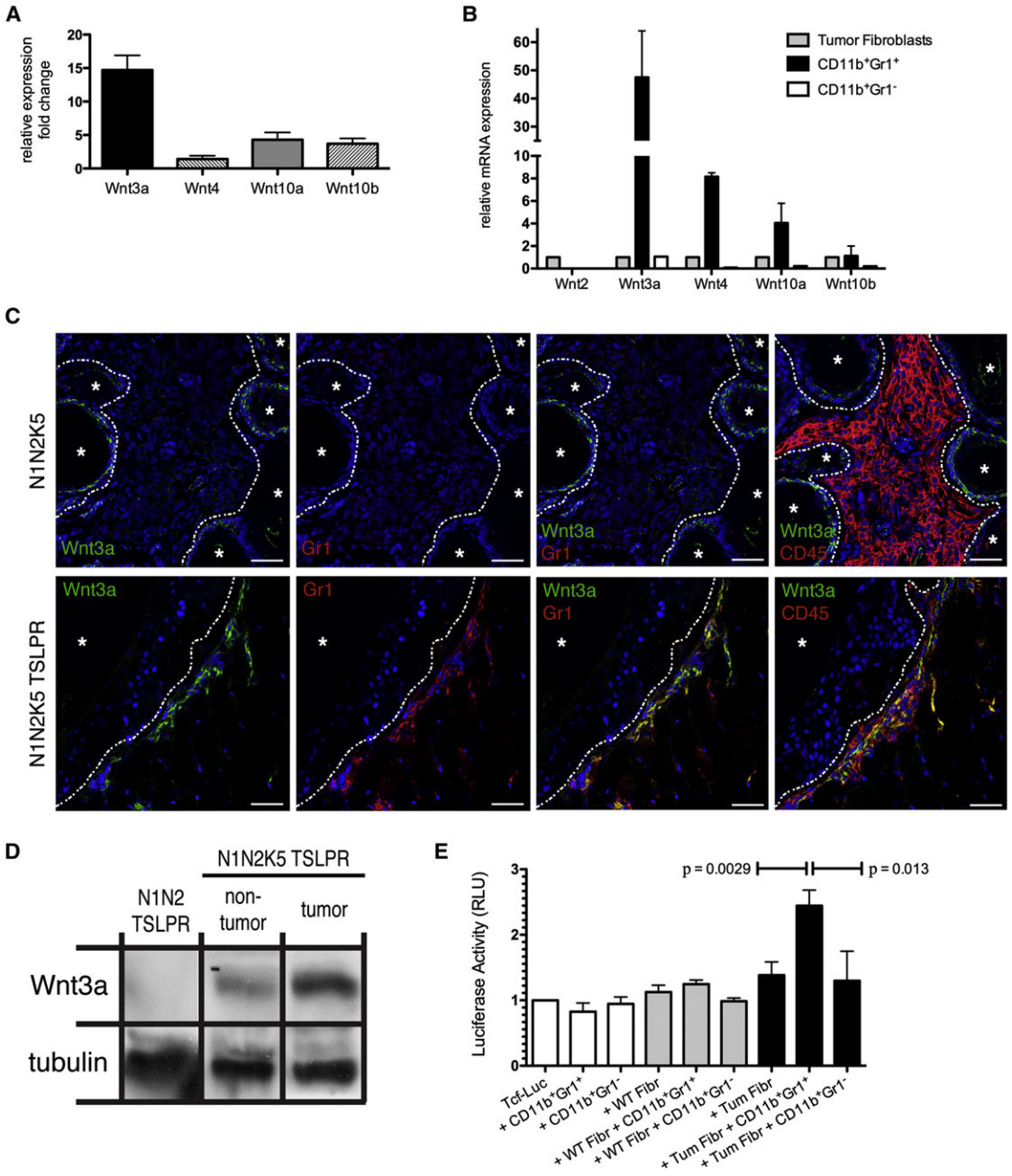

Figure 6. Tumor-Associated CD11b$^+$Gr1$^+$ Myeloid Cells Promote Tumor Development by Secreting Wnt Ligands

(A and B) Real-time PCR analysis for Wnt ligand expression performed on RNA isolated from whole-tumor-bearing N1N2K5 TSLPR skin (A) or specific cell populations isolated from the tumor microenvironment (B). In (A) gene expression is expressed relative to whole skin isolated from N1N2 TSLPR controls. In (B) gene expression is expressed relative to tumor-associated fibroblasts. Data represent the mean ± SD of three independent experiments.

(C) IF staining for Gr1, CD45, and WNT3a expression in the dermis of N1N2K5 and N1N2K5 TSLPR mice. Asterisks demarcate cyst lumen; dotted lines mark the border between the cystic epithelium and the surrounding dermis. The image shown for N1N2K5 skin displays a region with extensive CD45 staining to demonstrate the low proportions of Gr1$^+$ cells. Scale bars: 100 μm.

(D) Western blot analysis of WNT3a expression in whole-skin extracts from nontumor and tumor-bearing regions of N1N2K5 TSLPR mice. Tubulin was used as loading control; lanes shown are cropped from the same blot. The original blot is shown in Figure S5C.

(E) CD11b$^+$Gr1$^+$ and CD11b$^+$Gr1$^-$ myeloid cells were isolated from tumor-bearing skin of N1N2K5 TSLPR mice and cocultured with 293T cells expressing a Tcf-luciferase reporter (Tcf-Luc), with or without fibroblasts isolated from N1N2K5 TSLPR tumor-bearing skin (Tum Fibr) or WT dermis (WT Fibr). Luciferase activity was measured 36 hr after coculture (mean ± SD).

See also Figure S5.

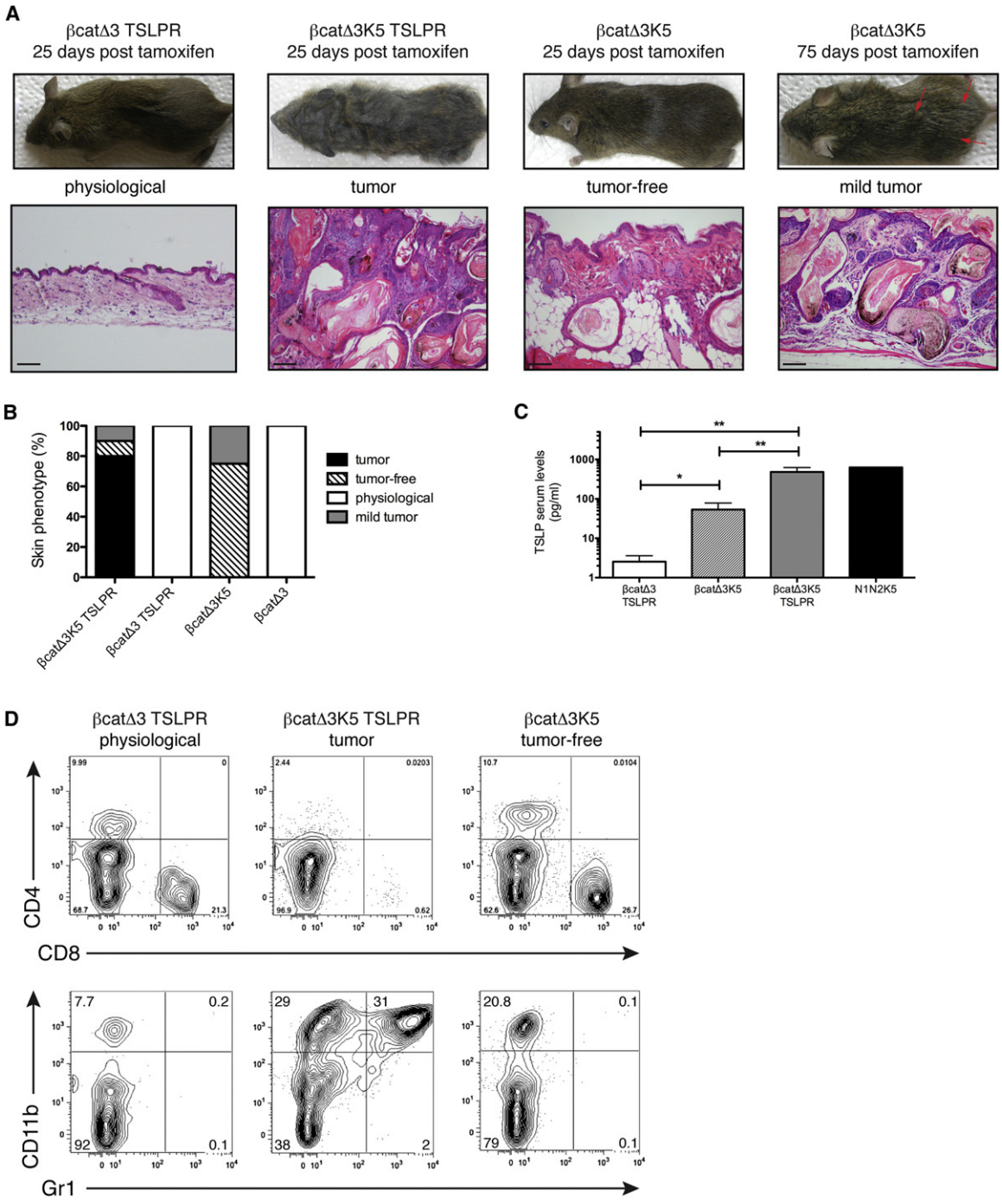

Figure 7. TSLP Mediates Protection against β-Catenin-Dependent Skin Carcinogenesis

(A) Representative images of βcatΔ3K5 (n = 5) and βcatΔ3K5 TSLPR (n = 10) mice after induction of activated β-catenin by five consecutive daily injections of tamoxifen starting at day P30. βcatΔ3 TSLPR mice were used as normal littermate controls (n = 8). A βcatΔ3K5 mouse is shown 75 days posttamoxifen to illustrate accelerated tumor development in the absence of TSLPR signaling. H&E staining performed on dorsal skin sections from each mouse are shown below each image. Arrows point to regions with overt skin phenotype. Scale bars: 100 μm.

(B) Bar diagram displaying the proportion of mice with the indicated skin phenotype 25 days after induction of activated B-catenin. Data represent the results of three independent experiments.

(C) TSLP serum levels were measured in βcatΔ3K5 TSLPR (n = 5), βcatΔ3 TSLPR (n = 3), βcatΔ3K5 (n = 4), and N1N2K5 (n = 3) mice 3 weeks after β-catenin activation or Notch inactivation at day P30. The bar diagram is the result of a single experiment run in triplicate (mean ± SD; *$p < 0.05$; **$p < 0.001$).

(D) Flow cytometric analysis of T cells and myeloid cells in the dermis of βcatΔ3 TSLPR control, βcatΔ3K5 TSLPR, and βcatΔ3K5 mice 30 days after induction of activated βcatenin. All data are gated on $CD45^+$ cells.

See also Figure S6.

manuscript by Demehri et al. (2012) in this issue of *Cancer Cell* also demonstrates that TSLP-dependent immune responses can protect against DMBA/TPA-induced tumors in a wild-type background. Importantly, this model is independent of any pre-existing genetic aberrations.

DISCUSSION

In this study, we have revealed a tumor protective role for the cytokine TSLP during cutaneous skin cancer development. This effect is primarily mediated by direct signaling on dermal $CD4^+$ and $CD8^+$ T cells via the TSLPR, which prevents the growth of β-catenin-dependent hair follicle tumors in Notch loss-of-function and β-catenin gain-of-function mouse models. Loss of TSLPR responsive T cells results in tumor development and is accompanied by the induction of protumorigenic inflammation, which augments Wnt/β-catenin signaling. These findings reveal a tumor-protective role for TSLP and demonstrate how acquired and innate arms of the immune system can mediate pro- and antitumor effects. This in turn may have broader implications with respect to the role of inflammation in other epithelial malignancies.

TSLP and T-Cell-Mediated Tumor Protection

A key finding in this study is that direct activation of the TSLPR on dermal $TCR\alpha\beta^+$ T cells elicits antitumor immune responses to cutaneous malignancies. The analysis performed in Notch mutant mice indicates that both $CD4^+$ and $CD8^+$ T cells mediate this protective effect, although $CD8^+$ T cells are the essential effector cells. That TSLP can mediate tumor protection by promoting $CD8^+$ T cell responses is surprising, as TSLP is considered to promote Th2-mediated immunity and thus is not normally associated with cytotoxic responses (Liu et al., 2007). However, it has been shown that TSLP can promote the development of cytotoxic $CD8^+$ T cells by inducing the differentiation of cytolytic effectors that express IL-5 and IL-13 (Soumelis and Liu, 2004). We also find that expression levels of IL-5 and IL-13 are elevated in N1N2K5 dermis (Dumortier et al., 2010), suggesting that TSLP induces a similar cytotoxic state in this model.

In addition, it appears likely that TSLP acts to maintain dermal T cells, as their proportions are significantly reduced upon TSLPR ablation. This is unlikely to be a consequence of impaired homing as Transwell migration studies indicate that $Tslpr^{-/-}$ T cells show normal migration (Figure S3F), consistent with a previous report (He et al., 2008). Activation of dermal T cells is also unaffected by loss of TSLPR (data not shown), suggesting that activation-associated proliferation is not perturbed. It is therefore likely that TSLP signaling promotes T cell survival by acting directly on $CD4^+$ and $CD8^+$ T lymphocytes, as demonstrated by earlier studies (Al-Shami et al., 2005; Rochman et al., 2007; Rochman and Leonard, 2008).

Regardless of the precise mechanism, the data presented here indicate that the tumor-protective role of TSLP is primarily mediated by a direct effect on dermal T cells. In support of this conclusion, the accompanying manuscript by Demehri et al. (2012) also demonstrates that TSLP elicits antitumor T cell immunity upon ablation of cutaneous Notch signaling. Interestingly, in their model $CD4^+$ T cells are sufficient for tumor protection and $CD8^+$ T cells are dispensable. This is likely due to the use of the *Msx2-Cre* deletor strain, which inactivates the Notch pathway during development and thus primes the developing immune system from an early time point. In our system, Notch deletion is induced only after birth, meaning that any T cell activity directed against epithelial tumor cells is a naive immunological response.

Induction of Protumorigenic Inflammation upon Loss of TSLPR

An important consequence of TSLPR ablation in the mouse models used in this study is the induction of protumorigenic inflammation, an important functional component of which are $CD11b^+Gr1^+$ myeloid cells. Why these cells accumulate in the dermis of N1N2K5 TSLPR mice but only represent a relatively minor population of myeloid cells in N1N2K5 animals is unclear and needs further investigation. One possible explanation is that the allergic response induced by TSLP is antagonistic to protumorigenic components of the inflammatory milieu. Such a mechanism has been proposed by a recent study indicating that histamine produced during allergic immune reactions prevents the accumulation of tumor-promoting immature $CD11b^+Gr1^+$ myeloid cells (Yang et al., 2011). In addition, we cannot formally exclude that the role of TSLP-responsive T cells is to act directly against $CD11b^+Gr1^+$ myeloid cells. However, we think this is unlikely based on the tumor-protective effect of TSLP demonstrated in βcatΔ3K5 mice, where tumor development occurs independently of myeloid cells.

An alternative explanation is that the $CD11b^+Gr1^+$ myeloid cells are recruited by putative cancer stem cells (CSCs) that secrete promyeloid factors. A recent study has demonstrated that $CD34^+$ cutaneous CSCs can induce a protumorigenic stroma via paracrine effects (Beck et al., 2011). We also observe expanded populations of immature $CD34^+$ epithelial cells in the tumors arising in N1N2K5 TSLPR mice (data not shown), suggesting similar mechanisms may be operating in the models used in this study.

Finally, it is possible that loss of TSLP-mediated immune responses results in increased loads of pathogenic organisms that may induce protumorigenic inflammation, as has been suggested by the link between specific infections and carcinogenesis (Parkin, 2006).

Wnt-Dependent Tumor Promotion by $CD11b^+Gr1^+$ Myeloid Cells

The tumor-promoting role of $CD11b^+Gr1^+$ myeloid cells has been reported previously by a variety of studies (Kowanetz et al., 2010; Qian et al., 2011; Rodriguez and Ochoa, 2008). Here, we demonstrate that these cells can exert this effect by augmenting Wnt/β-catenin signaling in neighboring epithelial cells via the secretion of Wnt ligands.

The ability of $CD11b^+Gr1^+$ myeloid cells to induce Wnt/β-catenin signaling is dependent on tumor-associated fibroblasts, which probably reflects increased expression of the Wnt potentiator POSTN. This suggests that the dermal stroma in these mice is primed to facilitate the protumorigenic function of $CD11b^+Gr1^+$ myeloid cells.

Because the recruitment of $CD11b^+Gr1^+$ cells is itself dependent on elevated β-catenin expression in the epidermis, it is likely that Wnt pathway activation is an early event during tumor

progression in the models described here. Indeed, loss of Notch receptors can increase levels of nuclear β-catenin in a cell autonomous manner (Devgan et al., 2005; Kwon et al., 2011). Therefore, we suggest that once recruited to the tumor stroma, myeloid populations can augment the Wnt signaling cascade and drive tumor growth. In this way, the epithelial population that initiates cancer development establishes a feed-forward loop that favors tumor progression.

Context-Dependent Role of TSLP during Cancer Development

The central theme of this study is the tumor-protective effect of TSLP during cutaneous cancer development. This is in contrast to previous reports that find TSLP can promote tumor growth and metastasis in mouse models of breast and pancreatic cancer (De Monte et al., 2011; Olkhanud et al., 2011; Pedroza-Gonzalez et al., 2011). The relevance of TSLP in this respect is indeed highlighted by the fact that pharmaceutical companies are seeking to develop drugs directed against TSLP (Edwards, 2008). However, within the human population, individuals who suffer from atopic allergic disorders have a reduced risk of developing certain types of cancer (Gandini et al., 2005; Prizment et al., 2007; Vajdic et al., 2009; Wang and Diepgen, 2005). It is tempting to speculate that the context in which TSLP functions as a tumor suppressor or tumor promoter is related to how allergic immune responses affect barrier versus glandular epithelial cells. It will be interesting to determine if TSLP-responsive T cells that induce allergic inflammation in other barrier epithelia, such as lung (Al-Shami et al., 2005), are also tumor protective.

Thus, whether TSLP is inducing a pro- or antitumorigenic immune response appears to be context- and tissue-dependent, and therefore blocking TSLP-mediated responses as a potential cancer treatment is a hypothesis that must be analyzed with caution.

EXPERIMENTAL PROCEDURES

Ethics Statement

All animal work was conducted in accordance with Swiss national guidelines. All mice were kept in the animal facility under EPFL animal care regulations. They were housed in individual cages at 23°C ± 1°C with a 12 hr light/dark cycle. All animals were supplied with food and water ad libitum. This study has been reviewed and approved by the Service Vétérinaire Cantonal of Etat de Vaud.

Mice

Notch1$^{lox/lox}$;*Notch2*$^{lox/lox}$;*K5Cre*^{ERT}, *Notch1*$^{lox/lox}$;*Notch2*$^{lox/lox}$;*Tslpr*$^{-/-}$;*K5Cre*^{ERT}, and *Tslpr*$^{-/-}$ mice were previously described (Dumortier et al., 2010). *Notch1*$^{lox/lox}$;*Notch2*$^{lox/lox}$;*Tslpr*$^{-/-}$;*K5Cre*^{ERT} mice were crossed to *Ctnnb1*$^{lox/lox}$ (Malanchi et al., 2008) mice to generate *Notch1*$^{lox/lox}$;*Notch2*$^{lox/lox}$; *Ctnnb1*$^{lox/lox}$;*Tslpr*$^{-/-}$;*K5Cre*^{ERT} mice. *Ctnnb1*$^{lox(ex3)}$ mice (Harada et al., 1999) were crossed with *Tslpr*$^{-/-}$ mice and *K5Cre*^{ERT} transgenic mice (Indra et al., 1999) to generate *Ctnnb1*$^{lox(ex3)}$;*Tslpr*$^{-/-}$;*K5Cre*^{ERT} mice. C57BL/6 CD45.1 (B6.SJL-Ptprc^{a}/BoyAiTac) and *Rag2*$^{-/-}$;$\gamma c^{-/-}$ (B6.Rag2^{tm1Fwa}Il2rg^{tmWjl}) mice were purchased from Taconic Europe (Germany). *Tslpr*$^{-/-}$ and *Rag2*$^{-/-}$ mice were crossed to C57BL/6 CD45.1 mice to obtain *Tslpr*$^{-/-}$ CD45.1 and *Rag2*$^{-/-}$ CD45.1 mice, respectively. *Jh*$^{-/-}$ (B6.129P2-Igh-J^{tm1Cgn}/J), *Cd4*$^{-/-}$ (B6.129S2-Cd4^{tm1Mak}/J), and *Cd8α*$^{-/-}$ (B6.129S2-Cd8a^{tm1Mak}/J) mice were purchased from the Jackson Laboratory (Bar Harbor, ME, USA). All mice used as donors in the bone marrow chimera and adoptive transfer experiments were on a pure C57BL/6 background. All Notch mutants were backcrossed >10 generations with C57BL/6 mice and thus can be considered to be on a pure C57BL/6 background. Depending on the experiment, gene inactivation was achieved by intraperitoneal injection at P6, P30, or P60 of control and floxed mutant mice with 1 mg/20 g body weight of tamoxifen (Sigma-Aldrich, St. Gallen, Switzerland) for five consecutive days.

Dermal Cell Isolation

Back skin was aseptically dissected from mice and incubated dermis-side down in a 1 mg/ml solution of collagenase/dispase (Roche, Indianapolis, IN, USA) for 1 hr at 37°C. The dermis was separated from the epidermis, dissociated mechanically, and incubated in a 2 mg/ml solution of collagenase (Sigma-Aldrich) for 45 min at 37°C with gentle agitation. Cell suspensions were filtered through a 70 μm cell strainer (BD Falcon, Franklin Lakes, NJ, USA) and washed twice in staining medium (1× HBSS/25 mM HEPES/2% newborn bovine calf serum).

Flow Cytometry

Single-cell suspensions were stained with monoclonal antibody conjugates in accordance with standard protocols and analyzed using a CyAn flow cytometer (Dako, Glostrup, Denmark). Data analysis and processing was performed using FlowJo software (Tree Star, Ashland, OR, USA).

Immunohistochemistry and Immunofluorescence

For immunohistochemistry, tissues were fixed in 4% PFA and embedded in paraffin. After sectioning, 4 μm sections were rehydrated, blocked with 3% H_2O_2, and incubated in antigen retrieval buffer (10 mM Tris/1 mM EDTA/0.05% Tween 20 [pH 9.0]) at 95°C for 20 min. Sections were then stained using unconjugated primary antibodies and the appropriate HRP-conjugated secondary antibodies. Staining was revealed by DAB (Sigma-Aldrich) revelation. For immunofluorescence, tissues were embedded in OCT compound and frozen. Cryosections (8 μm) were then fixed in acetone at 4°C for 2 min and air-dried for 20 min. After rinsing in PBS, sections were stained with unconjugated primary antibodies and the appropriate fluorophore-conjugated secondary antibodies. Fluorescent images were acquired using an LSM700 confocal microscope (Zeiss, Oberkochen, Germany).

See the Supplemental Experimental Procedures for further details.

SUPPLEMENTAL INFORMATION

Supplemental Information includes six figures, one table, and Supplemental Experimental Procedures and can be found with this article online at http://dx.doi.org/10.1016/j.ccr.2012.08.016.

ACKNOWLEDGMENTS

This work was supported in part by the Swiss National Science Foundation, the Swiss Cancer League, the Marie Curie Foundation, EuroSyStem, and OptiStem. We thank Rolf Kemler for providing the conditional *β-catenin* mice, Makoto Taketo for the conditional *β-catenin Δ3* mice, Pierre Chambon and Daniel Metzger for the *K5Cre*^{ERT} mice, Ursula Zimber-Strobl and Lothar Strobl for the conditional *Notch2* mice, and Warren Leonard for the *Tslpr*$^{-/-}$ mice. We thank Joerg Huelsken for providing the Wnt-reporter cells and reagents, Nicola Harris and Ilaria Mosconi for providing the TSLP-neutralizing antibody, and Daniel Hohl for the TEWL measurement apparatus. We would like to acknowledge Fabio Aloisio and Alessandra Piersigilli for pathological analysis of the tumors, Olivier Randin, Josè Artacho, Jessica Sordet-Dessimoz, and Gisèle Ferrand for technical assistance, and Miguel Garcia, Gonzalo Tapia, and Sintia Winkler for cell sorting. We thank Shadmehr Demehri and Raphael Kopan for discussion, sharing experimental data, and critical reading of the manuscript.

Received: February 8, 2012
Revised: June 8, 2012
Accepted: August 17, 2012
Published: October 15, 2012

REFERENCES

Agrawal, N., Frederick, M.J., Pickering, C.R., Bettegowda, C., Chang, K., Li, R.J., Fakhry, C., Xie, T.X., Zhang, J., Wang, J., et al. (2011). Exome sequencing of head and neck squamous cell carcinoma reveals inactivating mutations in NOTCH1. Science *333*, 1154–1157.

Al-Shami, A., Spolski, R., Kelly, J., Keane-Myers, A., and Leonard, W.J. (2005). A role for TSLP in the development of inflammation in an asthma model. J. Exp. Med. *202*, 829–839.

Allavena, P., Sica, A., Garlanda, C., and Mantovani, A. (2008). The Yin-Yang of tumor-associated macrophages in neoplastic progression and immune surveillance. Immunol. Rev. *222*, 155–161.

Aspord, C., Pedroza-Gonzalez, A., Gallegos, M., Tindle, S., Burton, E.C., Su, D., Marches, F., Banchereau, J., and Palucka, A.K. (2007). Breast cancer instructs dendritic cells to prime interleukin 13-secreting CD4+ T cells that facilitate tumor development. J. Exp. Med. *204*, 1037–1047.

Beck, B., Driessens, G., Goossens, S., Youssef, K.K., Kuchnio, A., Caauwe, A., Sotiropoulou, P.A., Loges, S., Lapouge, G., Candi, A., et al. (2011). A vascular niche and a VEGF-Nrp1 loop regulate the initiation and stemness of skin tumours. Nature *478*, 399–403.

Coussens, L.M., and Werb, Z. (2002). Inflammation and cancer. Nature *420*, 860–867.

De Monte, L., Reni, M., Tassi, E., Clavenna, D., Papa, I., Recalde, H., Braga, M., Di Carlo, V., Doglioni, C., and Protti, M.P. (2011). Intratumor T helper type 2 cell infiltrate correlates with cancer-associated fibroblast thymic stromal lymphopoietin production and reduced survival in pancreatic cancer. J. Exp. Med. *208*, 469–478.

Demehri, S., Liu, Z., Lee, J., Lin, M.H., Crosby, S.D., Roberts, C.J., Grigsby, P.W., Miner, J.H., Farr, A.G., and Kopan, R. (2008). Notch-deficient skin induces a lethal systemic B-lymphoproliferative disorder by secreting TSLP, a sentinel for epidermal integrity. PLoS Biol. *6*, e123.

Demehri, S., Turkoz, A., and Kopan, R. (2009). Epidermal Notch1 loss promotes skin tumorigenesis by impacting the stromal microenvironment. Cancer Cell *16*, 55–66.

Demehri, S., Turkoz, A., Manivasagam, S., Yockey, L.J., Turkoz, M., and Kopan, R. (2012). Elevated epidermal thymic stromal lymphopoietin levels prevent skin tumorigenesis. Cancer Cell *22*, this issue, 494–505.

Devgan, V., Mammucari, C., Millar, S.E., Brisken, C., and Dotto, G.P. (2005). p21WAF1/Cip1 is a negative transcriptional regulator of Wnt4 expression downstream of Notch1 activation. Genes Dev. *19*, 1485–1495.

Dumortier, A., Durham, A.D., Di Piazza, M., Vauclair, S., Koch, U., Ferrand, G., Ferrero, I., Demehri, S., Song, L.L., Farr, A.G., et al. (2010). Atopic dermatitis-like disease and associated lethal myeloproliferative disorder arise from loss of Notch signaling in the murine skin. PLoS ONE *5*, e9258.

Edwards, M.J. (2008). Therapy directed against thymic stromal lymphopoietin. Drug News Perspect. *21*, 312–316.

Fridlender, Z.G., Sun, J., Kim, S., Kapoor, V., Cheng, G., Ling, L., Worthen, G.S., and Albelda, S.M. (2009). Polarization of tumor-associated neutrophil phenotype by TGF-beta: "N1" versus "N2" TAN. Cancer Cell *16*, 183–194.

Gabrilovich, D.I., and Nagaraj, S. (2009). Myeloid-derived suppressor cells as regulators of the immune system. Nat. Rev. Immunol. *9*, 162–174.

Gandini, S., Lowenfels, A.B., Jaffee, E.M., Armstrong, T.D., and Maisonneuve, P. (2005). Allergies and the risk of pancreatic cancer: a meta-analysis with review of epidemiology and biological mechanisms. Cancer Epidemiol. Biomarkers Prev. *14*, 1908–1916.

Gat, U., DasGupta, R., Degenstein, L., and Fuchs, E. (1998). De Novo hair follicle morphogenesis and hair tumors in mice expressing a truncated beta-catenin in skin. Cell *95*, 605–614.

Hanahan, D., and Weinberg, R.A. (2011). Hallmarks of cancer: the next generation. Cell *144*, 646–674.

Harada, N., Tamai, Y., Ishikawa, T., Sauer, B., Takaku, K., Oshima, M., and Taketo, M.M. (1999). Intestinal polyposis in mice with a dominant stable mutation of the beta-catenin gene. EMBO J. *18*, 5931–5942.

He, R., Oyoshi, M.K., Garibyan, L., Kumar, L., Ziegler, S.F., and Geha, R.S. (2008). TSLP acts on infiltrating effector T cells to drive allergic skin inflammation. Proc. Natl. Acad. Sci. USA *105*, 11875–11880.

Indra, A.K., Warot, X., Brocard, J., Bornert, J.M., Xiao, J.H., Chambon, P., and Metzger, D. (1999). Temporally-controlled site-specific mutagenesis in the basal layer of the epidermis: comparison of the recombinase activity of the tamoxifen-inducible Cre-ER(T) and Cre-ER(T2) recombinases. Nucleic Acids Res. *27*, 4324–4327.

Jagelman, D.G. (1991). Extra-colonic manifestations of familial adenomatous polyposis. Oncology (Williston Park) *5*, 23–27, discussion 31–6.

Kowanetz, M., Wu, X., Lee, J., Tan, M., Hagenbeek, T., Qu, X., Yu, L., Ross, J., Korsisaari, N., Cao, T., et al. (2010). Granulocyte-colony stimulating factor promotes lung metastasis through mobilization of Ly6G+Ly6C+ granulocytes. Proc. Natl. Acad. Sci. USA *107*, 21248–21255.

Kwon, C., Cheng, P., King, I.N., Andersen, P., Shenje, L., Nigam, V., and Srivastava, D. (2011). Notch post-translationally regulates β-catenin protein in stem and progenitor cells. Nat. Cell Biol. *13*, 1244–1251.

Liu, Y.J., Soumelis, V., Watanabe, N., Ito, T., Wang, Y.H., Malefyt, Rde.W., Omori, M., Zhou, B., and Ziegler, S.F. (2007). TSLP: an epithelial cell cytokine that regulates T cell differentiation by conditioning dendritic cell maturation. Annu. Rev. Immunol. *25*, 193–219.

Malanchi, I., Peinado, H., Kassen, D., Hussenet, T., Metzger, D., Chambon, P., Huber, M., Hohl, D., Cano, A., Birchmeier, W., and Huelsken, J. (2008). Cutaneous cancer stem cell maintenance is dependent on beta-catenin signalling. Nature *452*, 650–653.

Malanchi, I., Santamaria-Martínez, A., Susanto, E., Peng, H., Lehr, H.A., Delaloye, J.F., and Huelsken, J. (2012). Interactions between cancer stem cells and their niche govern metastatic colonization. Nature *481*, 85–89.

Nicolas, M., Wolfer, A., Raj, K., Kummer, J.A., Mill, P., van Noort, M., Hui, C.C., Clevers, H., Dotto, G.P., and Radtke, F. (2003). Notch1 functions as a tumor suppressor in mouse skin. Nat. Genet. *33*, 416–421.

Olkhanud, P.B., Rochman, Y., Bodogai, M., Malchinkhuu, E., Wejksza, K., Xu, M., Gress, R.E., Hesdorffer, C., Leonard, W.J., and Biragyn, A. (2011). Thymic stromal lymphopoietin is a key mediator of breast cancer progression. J. Immunol. *186*, 5656–5662.

Parkin, D.M. (2006). The global health burden of infection-associated cancers in the year 2002. Int. J. Cancer *118*, 3030–3044.

Pedroza-Gonzalez, A., Xu, K., Wu, T.C., Aspord, C., Tindle, S., Marches, F., Gallegos, M., Burton, E.C., Savino, D., Hori, T., et al. (2011). Thymic stromal lymphopoietin fosters human breast tumor growth by promoting type 2 inflammation. J. Exp. Med. *208*, 479–490.

Prizment, A.E., Folsom, A.R., Cerhan, J.R., Flood, A., Ross, J.A., and Anderson, K.E. (2007). History of allergy and reduced incidence of colorectal cancer, Iowa Women's Health Study. Cancer Epidemiol. Biomarkers Prev. *16*, 2357–2362.

Proweller, A., Tu, L., Lepore, J.J., Cheng, L., Lu, M.M., Seykora, J., Millar, S.E., Pear, W.S., and Parmacek, M.S. (2006). Impaired notch signaling promotes de novo squamous cell carcinoma formation. Cancer Res. *66*, 7438–7444.

Qian, B.Z., Li, J., Zhang, H., Kitamura, T., Zhang, J., Campion, L.R., Kaiser, E.A., Snyder, L.A., and Pollard, J.W. (2011). CCL2 recruits inflammatory monocytes to facilitate breast-tumour metastasis. Nature *475*, 222–225.

Quezada, S.A., Peggs, K.S., Simpson, T.R., and Allison, J.P. (2011). Shifting the equilibrium in cancer immunoediting: from tumor tolerance to eradication. Immunol. Rev. *241*, 104–118.

Rochman, I., Watanabe, N., Arima, K., Liu, Y.J., and Leonard, W.J. (2007). Cutting edge: direct action of thymic stromal lymphopoietin on activated human CD4+ T cells. J. Immunol. *178*, 6720–6724.

Rochman, Y., and Leonard, W.J. (2008). The role of thymic stromal lymphopoietin in CD8+ T cell homeostasis. J. Immunol. *181*, 7699–7705.

Rodriguez, P.C., and Ochoa, A.C. (2008). Arginine regulation by myeloid derived suppressor cells and tolerance in cancer: mechanisms and therapeutic perspectives. Immunol. Rev. *222*, 180–191.

Sanders, P.G., Muñoz-Descalzo, S., Balayo, T., Wirtz-Peitz, F., Hayward, P., and Arias, A.M. (2009). Ligand-independent traffic of Notch buffers activated Armadillo in Drosophila. PLoS Biol. *7*, e1000169.

Soumelis, V., and Liu, Y.J. (2004). Human thymic stromal lymphopoietin: a novel epithelial cell-derived cytokine and a potential key player in the induction of allergic inflammation. Springer Semin. Immunopathol. *25*, 325–333.

Stransky, N., Egloff, A.M., Tward, A.D., Kostic, A.D., Cibulskis, K., Sivachenko, A., Kryukov, G.V., Lawrence, M.S., Sougnez, C., McKenna, A., et al. (2011). The mutational landscape of head and neck squamous cell carcinoma. Science *333*, 1157–1160.

Vajdic, C.M., Falster, M.O., de Sanjose, S., Martínez-Maza, O., Becker, N., Bracci, P.M., Melbye, M., Smedby, K.E., Engels, E.A., Turner, J., et al. (2009). Atopic disease and risk of non-Hodgkin lymphoma: an InterLymph pooled analysis. Cancer Res. *69*, 6482–6489.

Wang, H., and Diepgen, T.L. (2005). Is atopy a protective or a risk factor for cancer? A review of epidemiological studies. Allergy *60*, 1098–1111.

Wang, N.J., Sanborn, Z., Arnett, K.L., Bayston, L.J., Liao, W., Proby, C.M., Leigh, I.M., Collisson, E.A., Gordon, P.B., Jakkula, L., et al. (2011). Loss-of-function mutations in Notch receptors in cutaneous and lung squamous cell carcinoma. Proc. Natl. Acad. Sci. USA *108*, 17761–17766.

Weng, A.P., and Aster, J.C. (2004). Multiple niches for Notch in cancer: context is everything. Curr. Opin. Genet. Dev. *14*, 48–54.

Yang, X.D., Ai, W., Asfaha, S., Bhagat, G., Friedman, R.A., Jin, G., Park, H., Shykind, B., Diacovo, T.G., Falus, A., and Wang, T.C. (2011). Histamine deficiency promotes inflammation-associated carcinogenesis through reduced myeloid maturation and accumulation of CD11b+Ly6G+ immature myeloid cells. Nat. Med. *17*, 87–95.

Ziegler, S.F. (2010). The role of thymic stromal lymphopoietin (TSLP) in allergic disorders. Curr. Opin. Immunol. *22*, 795–799.